Shape change of tensegrity structures : design and control

Please check the document version of this publication:

Shape Change of Tensegrity Structures: Design and Control

Jeroen van de Wijdeven

Department of Mechanical Engineering

Technische Universiteit Eindhoven

P.O. Box 513, 5600 MB Eindhoven

The Netherlands

J.J.M.v.d.Wijdeven@tue.nl

Bram de Jager

Department of Mechanical Engineering

Technische Universiteit Eindhoven

P.O. Box 513, 5600 MB Eindhoven

The Netherlands

A.G.de.Jager@wfw.wtb.tue.nl

Abstract— **This paper focusses on shape changes of tensegrity structures. An optimization method is developed for design of a reference trajectory for shape changes of an arbitrary tensegrity structure. By defining an objective and constraints related to the shape change, constrained optimization is used to determine the reference trajectory. To improve suppression of vibrations during the shape change, an $\mathcal{H}_2$ controller is used in a feedback loop. To illustrate the use of the optimization method and selected control strategy, a shape change is simulated and the results are presented.**

I. INTRODUCTION

Tensegrity structures are built up from bars and tendons (strings), where bars are placed discontinuously in a continuous network of tendons [1], [2], [3]. While tendons can only handle tensile forces, bars can be subjected to both tensile and compressive forces. Int*egrity* (stability) of the tensegrity structure is obtained through pre-stress (*tens*ion) of the tendons, hence the word *tensegrity*.

In a Class 1 tensegrity structure the bars only connect to tendons, while in a Class 2 tensegrity structure the ends of two bars can be connected, together with a number of tendons, in a single joint or node.

Shape changes of a tensegrity structure can be accomplished by altering the rest length of the elements in the structure. Though both bars and tendons can be used, in this paper it is assumed that bars are passive elements, i.e., their lengths cannot be actively altered.

The possibility to actively change the shape of tensegrity structures makes these structures an interesting alternative for current structures used in space applications, e.g., deployable antennas or radio telescopes, or in medical applications, e.g., minimal invasive surgery. In [4] changes in rest length of tendons are used for deployment of a Class 1 tensegrity structure. Using time optimal control, the rest lengths are determined by optimizing a single shape dependent parameter. Shape changes of a specific Class 2 tensegrity structure are worked out in [5], using again time optimal control.

To suppress vibrations in a structure, a controller can be included in the feedback loop. In [6] control of a tensegrity structure has been accomplished using LQG, neural networks, and Gain Scheduling Control. In [4] and [5] feedback linearization is applied for shape control of tensegrity structures. In [7] and [8] suppression of vibrations is accomplished in a smart antenna and a laminate beam respectively, using $\mathcal{H}_2$ control.

The methods for design of reference signals for shape changes discussed in [4] and [5] are only valid for specific groups of tensegrity structures. The contribution of this paper is the introduction of an optimization method for shape changes of *arbitrary* tensegrity structures. The benefit of optimization is the freedom to influence the design outcome with constraints.

Due to the freedom to select and to adjust control objectives, $\mathcal{H}_2$ control will be applied for vibration suppression during the shape change.

The paper is organized as follows: First a method for design of a reference trajectory for arbitrary tensegrity structures is discussed. Then design of the $\mathcal{H}_2$ controller is worked out and the overall control scheme is presented. To illustrate the methods developed, an example of a shape change with a two dimensional tensegrity structure is given. This paper finishes with conclusions and remarks.

II. REFERENCE TRAJECTORY

Before going into detail on reference trajectories, let us first clarify some notations used to describe a tensegrity structure: Lengths of bars are represented by L_b, the length of stressed tendons is given by L_t and corresponding force by $F_t(> 0)$, while for unstressed tendons it is L_{t0} and $F_t = 0$. Forces in bars are represented by F_b. The length of element i can be determined using $L_i = ||p_{2_i} - p_{1_i}||$, with $|| \cdot ||$ the Euclidean norm of $\cdot$ and p_{1_i} and p_{2_i} the coordinates of the two nodes of element i. The vector p contains all nodal positions: $p = [p_1^T, \ldots, p_{2n_b}^T]^T$, with n_b the total number of bars in the structure.

Assumptions used throughout the paper are: bars are considered rigid, i.e., infinitely stiff, and the joints are frictionless. These assumptions result in relatively simple systems for which a simple model can be derived, because no bending forces are present in the system.

To perform a shape change, i.e., a change in geometry, a corresponding reference trajectory, p_{ref}, for the nodal positions of the tensegrity structure is needed. These reference signals can be obtained by solving an optimization problem. Due to the number of nodes in a non-trivial structure, the optimization will be a larger scale one. It will also be non-convex and nonlinear.

In [9] feasibility of truss structures is verified using optimization and in [10] optimization is applied to find optimal mass to stiffness for tensegrity structures by adapting the

geometry. Approaches presented in [9] and [10] are useful for the design of reference trajectories for shape changes.

The optimization problem consists of minimizing an objective J, subject to constraints C:

$$p_{ref} = \arg\min_p \ J(p), \quad \text{sub} \quad C(p) \leq 0. \quad (1)$$

Due to the scale of the problem, no dynamics are included in the constraints. Dynamic effects will be handled by the feedback controller.

To obtain an actual reference trajectory, the desired shape change and time span are divided into N sub-shape changes and time steps using gridding. At every time step on the total time span, the sub-shape change is optimized while the constraints are met. When all the N optimizations are feasible, they result in (sub-)optimal values for the design variables and a total shape change that is obtained by carrying out the sub-shape changes sequentially.

The constraints related to shape changes of tensegrity structures are:

Geometry related constraints. There are a number of constraints related to geometry of the tensegrity structure. The first constraint is related to fixed coordinates of nodal positions, e.g., by a support

$$A_{joint}p - p_{joint} = 0. \quad (2)$$

The nodal positions are represented by vector p, A_{joint} is a sparse matrix filled with zeros and ones, and the vector p_{joint} contains the coordinates of the fixed nodal positions, the supported ends of bars.

The constraint related to shapes defined by desired positions of nodes is given by

$$A_{des}p - p_{des} = 0, \quad (3)$$

which is similar to (2). The matrix A_{des} is again a sparse matrix and p_{des} contains the desired nodal positions, which can be a function of time in this constraint.

It is possible that a shape is not specified by desired positions, but by a shape function. Dependent on one or more coordinates of a node, the other coordinate(s) are determined so that the node is positioned on the desired shape. The corresponding constraint is

$$f(p) = 0. \quad (4)$$

The bars are assumed to be rigid and should thus not change length. The related constraint is given by

$$L_b - L_{b_0} = 0. \quad (5)$$

It illustrates that the current bar lengths L_b must be equal to the initial bar lengths L_{b_0}.

A final constraint is found in defining a minimum length of the tendons

$$L_{t_{min}} - L_t \leq 0. \quad (6)$$

This minimum length corresponds to the minimum allowable distance between nodes connected by tendons, and prevents nodes from colliding.

Force related constraints. The most important force constraint is related to integrity of the tensegrity structure. A sufficient condition to guarantee integrity is to state that all forces in the tendons must be positive, i.e., under tension. Static equilibrium forces in the tendons, F_t, are not unique, due to pre-stress, and can be determined using a quadratic programming formulation:

$$F_t = \arg\min_{f_t} \quad f_t^T f_t, \quad (7)$$

$$\text{sub} \quad A_{eq}(p)f_t = b_{eq}(p) \quad (8)$$

$$f_t \geq \alpha > 0, \quad (9)$$

with α the minimum allowed tension in the tendons. The matrix $A_{eq}(p)$ and vector $b_{eq}(p)$ are found by stating the equilibrium conditions for forces and moments. Bar forces can be determined by summation of the different tendon forces and external forces in free nodes of the bars.

Note that F_t is determined using optimization. Thus, the tendon forces are obtained by solving an optimization problem inside another (larger) optimization, see Fig. (1). When solving (1) feasibility of F_t from (7)-(9) is assumed (but not guaranteed). Problem (1) and (7)-(9) could be combined. However, the separation gives a better view of the structure of the optimization problem.

Since only elastic deformation of tendons is desired, the forces in the tendons should remain smaller than the yield force:

$$F_t - \kappa_t F_{t,yield} \leq 0, \quad (10)$$

with κ_t a safety gain, $0 < \kappa_t \leq 1$.

To avoid permanent damage to the bars, forces are not allowed to surpass the yield and buckling force. Since dominant forces in the bars F_b are compressive (negative), the corresponding constraints are:

$$\kappa_b F_{b,yield} - F_b \leq 0 \text{ or } \kappa_b F_{b,buck} - F_b \leq 0 \quad (11)$$

Only the most stringent constraint in (11) will have to be included in the optimization problem of (1). The less stringent constraint is then automatically met.

The final force related constraints correspond to the maximal allowed changes in forces, ΔF, from sub-shape $k-1$ to sub-shape k

$$F_k - F_{k-1} - \Delta F \leq 0 \text{ and } -\Delta F - F_k - F_{k-1} \leq 0. \quad (12)$$

Limiting ΔF limits excitation of modes at higher frequencies in the structure.
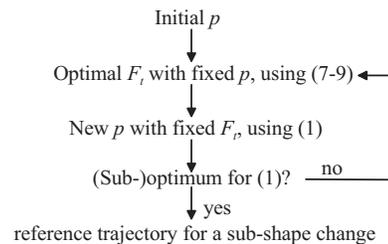

Fig. 1. Optimization scheme for one sub-shape change

In (12) $F_k = [F_{t_k}^T, \; F_{b_k}^T]^T$ and F_0 corresponds to the initial element forces.

Other constraints. During the shape change, elements, i.e., bars and tendons, are not allowed to collide. If collision would occur, the shape change could not be feasible.

The objective of the optimization is not determined beforehand. Depending on what is desirable during the shape change, the objective can be related to element forces, control effort, energy consumption, etc. In this paper the decision has been made to focuss on the control effort. Minimizing the control effort can be done by minimizing changes in tendon length between two steps in the shape change. The objective is then:

$$J = \left(L_{t_k} - L_{t_{k-1}}\right)^T \left(L_{t_k} - L_{t_{k-1}}\right), \qquad (13)$$

with k denoting the current time step in the shape change.

Though different design variables can be used in the optimization problem, the nodal positions p have been selected as design variable. They result in the least complicated problem definition, i.e., the largest number of linear constraints and the smallest number of nonlinear constraints.

When feasible, the output of the optimization problem contains the nodal positions p_{ref}. However, for the shape change the rest length of the tendons L_{t0} are required. To obtain $L_{t0,ref}$, first (7)-(9) is applied to determine the (static) tendon forces F_t during the shape change. Applying the constitutive equation

$$F_t = \frac{EA_t}{L_{t0,ref}} \left(L_t(p_{ref}) - L_{t0,ref}\right), \qquad (14)$$

the rest lengths can be determined. In (14) E denotes Young's modulus of the material used for tendons and A_t the cross sectional area of the tendons.

III. SHAPE CONTROL

Depending on the material used for the tendons, a tensegrity structure can have little damping. When the reference trajectory is only used for feedforward control, this lack of damping can lead to poorly damped structural vibrations during and after the shape change. To reduce vibrations an $\mathcal{H}_2$ controller is introduced in a feedback loop.

The $\mathcal{H}_2$ control strategy is based on a linear model of a system. The dynamics of tensegrity structures are however nonlinear. This is due to the nonlinear description of the orientation of the bars in the structure, and the fact that tendons can only handle tensile forces. The latter results in modeling of tendons as one-sided springs. Furthermore, large displacements occur during shape changes, making a linearized model inaccurate for simulations. It is beyond the scope of this paper to present the actual dynamic equations, though they can simply be derived using Lagrange, e.g., [5], or by Newton-Euler equations, e.g., [11].

The nonlinear dynamics are schematically presented by:

$$\dot{x} = f(x, u) \text{ and } y = g(x, u) \qquad (15)$$
$$x \in \mathbb{R}^{2N_{DOF}}, \; u \in \mathbb{R}^{n_t}$$

In (15) x corresponds to the states of the system, u to the input, i.e., the rest length of all n_t tendons, and y to the output of the system. The degrees of freedom (DOFs) of the structure equal N_{DOF}.

To be able to apply $\mathcal{H}_2$ control to tensegrity structures, the dynamics are linearized. The result is a model P in state space representation:

$$P: \qquad \dot{\tilde{x}} = A\tilde{x} + B\tilde{u}, \; \tilde{y} = C\tilde{x} + D\tilde{u} \qquad (16)$$
$$\tilde{x} = x - x_0, \; \tilde{u} = u - u_0, \; \tilde{y} = y - y_0,$$

where $\cdot_0$ indicates the stable equilibrium around which the linearization has been performed.

For the design of the $\mathcal{H}_2$ controller a number of issues have to be discussed:

Measurement variable. For measurements a number of variables can be used, e.g., the stressed length of the tendons, tendon forces or nodal positions. In this paper it has been decided to use nodal positions as measurements.

Disturbances. Two disturbances are included in the design of the controller. The first disturbance, w, represents uncertainties in the actuator dynamics. The second disturbance v represents measurement noise.

Controller input. The input into the controller is selected to contain the errors in nodal positions, $e = p_{ref} - p$. Since measurement noise is present in the system, the actual input equals $e + v$.

Control objectives. A first objective is related to the desire to suppress vibrations. Implementing this objective in the controller design results in the goal to minimize the error in nodal positions and its derivatives. A second objective is found in minimizing the control effort u. For tensegrity structures there is a third objective that is of great importance: the desire to maintain integrity of the structure during and after the shape change. To accomplish this, a sufficient condition is defined stating that the difference between the reference tendon forces $F_{t,ref}$ and the actual tendon forces F_t should be smaller than α of (9), i.e., minimize $F_{t,ref} - F_t$.

Weighting filters. All the external inputs and control objectives are subjected to filtering. The input filters V_i are selected to approximate the spectrum of the input signals, while the output filters W_i are designed to emphasize the relevant frequencies of the objectives.

For the design of the controller an augmented plant P_{aug} of the system is needed. The final augmented plant, including the issues discussed in this section, is presented in Fig. 2. Here W contains the external inputs, U the controller output, Z the control objectives, and Y the controller input. With the $\mathcal{H}_2$ controller designed, the final system can be defined. The closed loop system is given in Fig. 3, with C referring to the $\mathcal{H}_2$ controller and TS to the nonlinear tensegrity structure, (15).

A note must be made about the stability analysis of the closed loop system. In this paper stability is studied locally
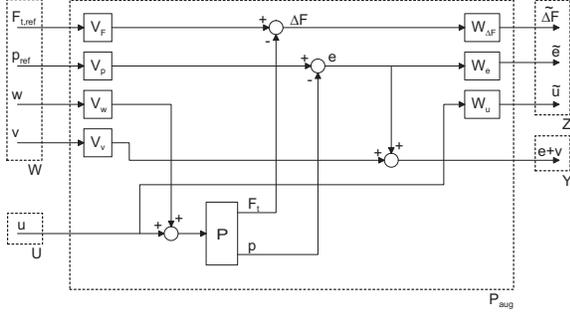
Fig. 2.   Augmented plant

Fig. 5.   Two dimensional tensegrity structure

by checking the positions of the poles of the *linearized* closed loop system around each of the N operating points on the trajectory, not only around x_0. However, global stability and robustness of the *non*linear closed loop system is still an open question.

The reference signals contain only a limited number (N) of operating points on the trajectory. To generate data between two operating points, linear interpolation of the reference signals is applied. When the interpolated $L_{t0,ref}$ and p_{ref} are used in (14) to determine the corresponding tendon forces, there is a relatively large decrease in tendon forces between two operating points, caused by linear interpolation of $L_{t0,ref}$ and p_{ref}. This is not desired, since decrease in tendon force can lead to loss of integrity of the tensegrity structure.

To avoid this problem, the control of Fig. 3 is changed to Fig. 4. Now, the linearly interpolated reference nodal positions p_{ref} and tendon forces $F_{t,ref}$ are used as reference signals. With p_{ref}, $F_{t,ref}$, and (17), the rest lengths of the tendons can be determined.

$$u_{ff} = L_{t0,ref} = \frac{L_t(p_{ref})}{\left(1 + \frac{F_{t,ref}}{EA_t}\right)} \qquad (17)$$

The benefit of Fig. 4 over Fig. 3 is that now there is a relatively smooth transition in the tendon forces throughout a sub-shape change instead of a smooth rest length of the tendons, making it easier to maintain integrity of the
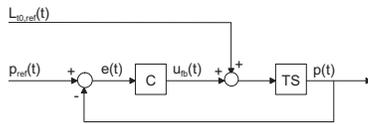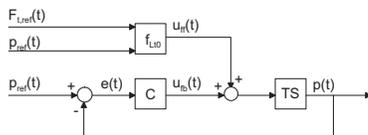

Fig. 3.   Closed loop system
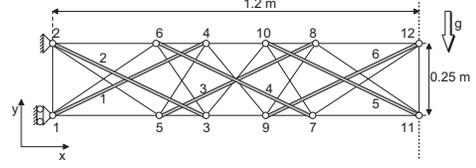

Fig. 4.   Adapted closed loop system

structure. Note, however, that moving from one operating point to the next still leads to discontinuous first derivatives due to the linearly interpolated reference trajectory. This will result in excitation of the structure.

IV. EXAMPLE

To illustrate the method for generating reference trajectories and to show the improvements of the shape change with shape control, an example with a two dimensional (2D) tensegrity structure is worked out. The steel structure under study is presented in Fig. 5, with g denoting the gravity vector. First the reference trajectory will be discussed, followed by simulations with feedforward and feedback control.

A. Reference trajectory design

For design of the reference trajectory the objective and constraints must be determined. Section II already discussed the objective of minimizing the control effort, leaving the topic of specifying the details of the constraints. Note that, since the tensegrity structure is 2D, the constraint of collision avoidance is irrelevant.

From Fig. 5 it follows that node 1 is restricted in y-direction and node 2 is fixed in both x- and y-direction. Furthermore, it is desired that nodes 11 and 12 do not move in the x-direction. These restrictions correspond to constraints (2) and (3) respectively.

For tendons the minimum length is set to $L_{t_{min}} = 0.05$ m, the diameter to 2mm, and the minimum and maximum allowed tendon forces to 0.06 and 0.7 times the yield force of the tendons. The bars are circular, symmetric, and hollow with diameters $d_{in} = 14$mm, $d_{out} = 20$mm. Since the buckling force of the bars is smaller than the yield force the maximum allowed bar force is related to the buckling force ($F_{b,max} = 0.7 F_{b,buck}$). Finally the maximum allowed change in force ΔF is set to 0.1 times the maximum allowed tendon force, i.e., to $0.07 F_{t,yield}$.

The shape the tensegrity structure has to follow is expressed in (18) and (19). All $2n_b$ nodes, with coordinates $p_i(t) = (x_i(t), y_i(t))$, $i = 1, \cdots, 2n_b$, must be positioned on this second order shape given by $y_i^*(t) = g(x_i(t))$. The corresponding constraint, (4), is $f_i(p) = y_i - y_i^* = 0$. For the lower nodes 1,3,5,7,9, and 11 $y_0^* = 0$, for the upper nodes $y_0^* = 0.25$. Fig. 6 a) gives a graphic interpretation of the shape and corresponding parameters.

$$r_1(t) = r_0(t) + \Delta r_1, \ r_2(t) = r_0(t) + \Delta r_2,$$
$$r_3(t) = r_0(t) + \Delta r_3 \qquad (18)$$
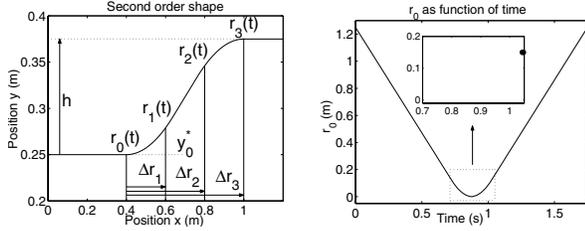
Fig. 6. a) Second order shape   b) r_0 as function of time

Fig. 8. Reference nodal positions p_{ref} and tendon forces $F_{t,ref}$

$$
\begin{aligned}
y_i^*(x_i) &= y_0^* && \text{for } x_i \leq r_0 \\
y_i^*(x_i) &= \tfrac{1}{2}A(x_i - r_0)^2 + y_0^* && \text{for } r_0 < x_i \leq r_1 \\
y_i^*(x_i) &= A\Delta r_1(x_i - r_1) + y_i^*(r_1) && \text{for } r_1 < x_i \leq r_2 \\
y_i^*(x_i) &= -\tfrac{1}{2}A(x_i - r_2)^2 + \\
&\quad + A\Delta r_1(x_i - r_2) + y_i^*(r_2) && \text{for } r_2 < x_i \leq r_3 \\
y_i^*(x_i) &= y_i^*(r_3) && \text{for } x_i > r_3
\end{aligned}
\tag{19}
$$

$$
\text{with } A = \frac{h}{\Delta r_1(r_3 - r_1)}
\tag{20}
$$

The shape "moves" with constant time steps and varying $r_0(t)$. For this example $r_0(t)$ is given in Fig. 6 b), from which it can be seen that the shape change is symmetric, resulting in a final shape equal to the initial shape. The motion represents moving the structure into a hollow, shaped like Fig. 7 step 55, and then withdrawing it.

Solving the optimization problem results in the shape change illustrated by Fig. 7. Although only 9 steps are presented, the actual number of steps in the shape change is $N = 110$. Due to symmetry in the shape change, only the first 55 steps have been determined. The second half of the shape change is equal to the first half, but reversed in sequence. The corresponding (symmetric) reference signals for the nodal positions and tendon forces are given by Fig. 8 in the upper and lower plot respectively. The first 1.75 seconds is used for the shape change, the final 0.25 seconds to let the system come to rest.

B. Shape control

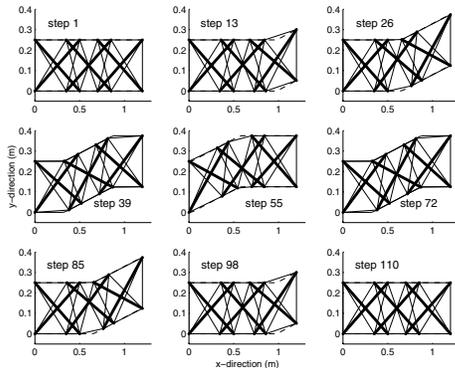The linear model P of the tensegrity structure contains 30 states, 22 inputs and 15 outputs and is obtained using

Fig. 9. Transfer functions of the linearized tensegrity structure
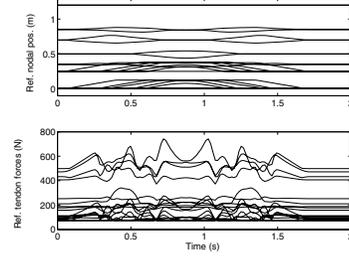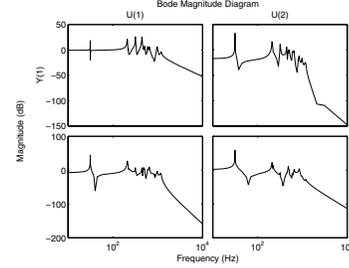
the initial configuration of the structure. The number of inputs equals the number of tendons in the structure, and the number of states relates to the number of DOFs in the structure, see (15). The outputs (nodal positions) are selected to be identical to the DOFs of the structure, i.e., $y \in \mathbb{R}^{N_{DOF}}$.

Fig. 9 presents the transfer functions of the first two inputs to the first two outputs. It can be seen from Fig. 9 that damping is included in the system. The dimensionless damping is assumed to be approximately between 0.001-0.01% and caused by the different elements in the structure, e.g., damping in tendons, and friction in actuators.

With the generated reference signals from Fig. 8, simulations have been done. Initially no feedback controller is applied, resulting in nodal position errors given in the first plot of Fig. 10. The errors remain acceptable up to around 0.8 s, after which larger oscillations start to occur. This behavior can be explained by the fact that the reference shape slows down towards the highest point, step 55, while inertia of the system forces the structure to move on. Since almost no damping is present in the structure, the vibrations hardly die out.

During the shape change some elongations of the tendons become negative, see the first plot of Fig. 11. This indicates that these tendons go slack, due to lack of tensile force. Since absence of pre-stress in tendons can jeopardize the integrity of the structure, it can be concluded that the use of only feedforward control is not sufficient to control shape changes of tensegrity structures.

Better results could be obtained using materials with a smaller Young's modulus or more damping, by increasing the time span of the shape change, or by applying feedback control. The latter results in the introduction of the $\mathcal{H}_2$
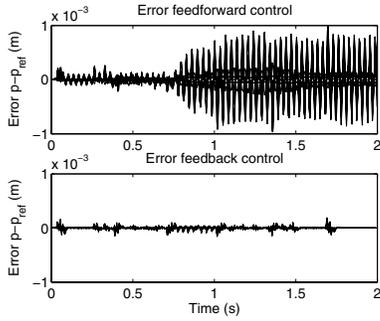

Fig. 7. Shape change of a tensegrity structure

Fig. 10. Nodal position errors $p - p_{ref}$ (m)

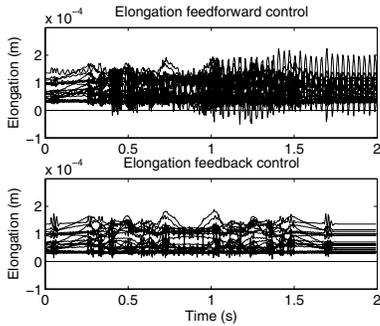
Fig. 11. Elongation of tendons $L_t - L_{t0}$(m)

controller. The controller is designed, using the specifications from section III. The control objectives related to the nodal position errors and tendon forces are weighted so that the amplitudes of the filtered $\tilde{e}$ and $F_{t,ref} - F_t$ are approximately equal at low frequencies. The objective concerning the control effort is chosen to be subordinate to the other two objectives so that the control effort is not the limiting factor in the error reduction. The linearized closed loop is stable for all N operating points of the trajectory, using a single controller designed for x_0.

Including the $\mathcal{H}_2$ controller in the feedback loop results in the nodal position errors given in the second plot of Fig. 10. Though small vibrations are still present (mainly caused by the discontinuous first derivatives of the reference signals) the dominant vibrations are successfully removed by the feedback controller. Furthermore, the elongations remain positive, Fig. 11 second plot, and thus pre-stress in the tendons is maintained.

The control effort needed to remove the vibrations corresponds to force corrections in the tendons up to about 5% of the pre-tension prescribed by the reference trajectory. Smaller stiffness of the tendons would result in larger changes in rest length. Implementation of the shape change on an experimental testbed can be difficult. The actuators responsible for the changes in tendon length must be able to cope with both small $O(10^{-5})$ and large $O(10^{-1})$ variations in tendon length, with high and low frequency contents respectively. This can, however, be achieved by a dual actuator setup.

V. CONCLUSIONS AND REMARKS

This paper presented a method for generating reference trajectories for arbitrary tensegrity structures. By defining an objective and several constraints, an optimization algorithm has been used to determine the reference signals. For suppression of vibrations and maintaining integrity of the tensegrity structure throughout the shape change an $\mathcal{H}_2$ controller is included in the control scheme. A two dimensional example is used to illustrate the presented methods.

A benefit of the proposed optimization algorithm is that adding or altering constraints and objective do not alter the structure of the algorithm.

A first remark is concerned with the global (robust) stability of the closed loop system. Checking stability of the linearized system around every operating point, as is done in this paper, only gives a first indication about stability of the nonlinear system. Global stability and robustness of the nonlinear closed loop system remains an open question.

In this paper all tendons in the structure are assumed to be active, i.e., can alter their rest length. This may, however, not be realizable in a testbed. It is possible to simply add passive tendons as extra constraints in the optimization problem for design of the reference trajectory. A more charming solution, however, can be found in [11], where a systematic method is employed for selecting the controller inputs and outputs.

REFERENCES

[1] K. Snelson, http://www.kennethsnelson.net
[2] http://www.mae.ucsd.edu/research/reskelton/laboratory/SSCL.htm
[3] Robert E. Skelton, J. William Helton, Rajesh Adhikari, Jean-Paul Pinaud, Waileung Chan, An Introduction to the Mechanics of Tensegrity Structures, In *The Mechanical Systems Design Handbook: Modeling, Measurement, and Control*, editors: Yildirim Hurmuzlu and Osita Nwokah, chapter 17, pp. 315-388, CRC Press, Boca Raton, 2002
[4] C. Sultan and R.E. Skelton, Deployment of Tensegrity Structures, *Int. Journal of Solids and Structures*, (40), pp. 4637-4657, 2003
[5] J.B. Aldrich, R.E. Skelton and K. Kreutz-Delgado, Control Synthesis for a Class of Light and Agile Robotic Tensegrity Structures, In: *Proc. of the American Control Conference*, pp. 5245-5251, Denver, Colorado USA, June 4-6 2003
[6] N. Kanchanasaratool, *Control of Flexible Structure*, PhD Thesis, The Australian National University, March 2003
[7] D.J. Leo and D.J. Inman, Optimal collocated control of a smart antenna, In: *Proc. of the 33rd IEEE Conference on Decision and Control*, pp. 109-114, Lake Buena Vista, Florida USA, December 1994
[8] D. Halim and S.O. Reza Moheimani, Experiments on spatial $\mathcal{H}_2$ control for vibration suppression of a piezoelectric laminate beam, In: *Proc. of the 40th IEEE Conference on Decision and Control*, pp. 3860-3865, Orlando, Florida USA, December 2001
[9] H.J. Schek, The Force Density Method for Form Finding and Computation of General Networks, *Computer Methods in Applied Mechanics and Engineering*, 3(1), pp. 115-134, January 1974
[10] B. de Jager, M. Masic and R.E. Skelton, Optimal Topology and Geometry for Controllable Tensegrity Systems, In: *IFAC, 15th Triennial World Congress*, Barcelona, Spain, 2002
[11] B. de Jager and R. Skelton, Input/Output Selection for Planar Tensegrity Models, In: *Proc. of the 40th IEEE Conference on Decision and Control*, pp. 4280-4285, Orlando, Florida USA, December 2001